

Delamination identification using machine learning methods and haar wavelets

Ljubov Feklistova, Helle Hein

Institute of Computer Science

University of Tartu, Liivi 2, 50409 Tartu, Estonia

e-mail: ljubov.feklistova@ut.ee, helle.hein@ut.ee

The present paper focuses on the identification of delamination size and location in homogeneous and composite laminates. The modal analysis methods are employed to calculate the data patterns. An aggregated approach combining Haar wavelets, support vector machines (SVMs) and artificial neural networks (ANNs) is used to solve identification problems. The usability and effectiveness of the proposed technique are tested by several numerical experiments. The advantages of the proposed method lie in the ability to make fast and accurate calculations.

Keywords: delamination identification, free vibrations, Euler-Bernoulli beam theory, Haar wavelets, machine learning methods.

1. INTRODUCTION

Laminate is a type of material made of two or more layers joined by an adhesive. The layers can be of the same material (laminated glass, plywood) or different (a sheet of glass sandwiched between plastic). Due to the advanced properties of combined materials, laminates and composites are frequently used in the contemporary civil engineering and heavy machinery. However, cutting laminates or severe conditions of performance (oscillating load, strain, stress, impact of foreign objects) can force the layers to stratify. This process is known as delamination. An early detection and continuous monitoring of delamination for the growth and location help avoid significant financial losses and emergency situations.

Nowadays monitoring is carried out using actuators or damage detection sensors based on piezoelectric effect, acoustic emission, strain gauge force, temperature measurement, etc. [1–3]. Pressure, strain and force can be measured quite precisely. Nevertheless, the techniques are not risk free: voltage unbalance degrades motor efficiency, causes rotor losses, increases temperature [4]; emerging electrical field or resonance occasionally causes structural damage to the surface [3, 5].

Conventional techniques based on vibration analysis (e.g., Fast Fourier Transform) are not sufficiently expedient to analyze signals with transitory characteristics. Such methods depend on the machine load and require high-resolution data [6]. Despite these disadvantages, machine vibration is still the best indicator of a structure's overall technical condition [4, 6]. It can be used as one of the first detectors, classifiers and reporters of emerging defects since each mechanical fault, including delamination, generates vibrations in its own specific frequency domain [6].

The problem of high-resolution data can be overcome with the aid of wavelet analysis. The latter is a space and time scaled representation of signals. In contrast to the harmonic orthogonal functions, which change periodically over the entire range of arguments, wavelets have non-zero values only on a limited part of the interval. They are applied for the signals of short duration and finite energy functions, which are local in time and frequency. Hereof, the wavelet analysis consists of multiplication of the signal, presented as a time function, with a wavelet function, and then the

transform is computed for each analyzed segment. As a result, the function is represented in terms of variations, localized on two independent variables - frequency and time position of pulse (time). The information content, presented in the initial form of the signal, is not altered [7]. The choice of the wavelet function in practical applications is based on trial and error since there is no known unique wavelet that could satisfy all structural health monitoring (SHM) needs [8].

Following to the nature of the signal, wavelet transforms can be classified as discrete and continuous wavelet transforms. The former decomposes digital signals into wavelet and scaling coefficients; the latter divides a continuous-time function into wavelets derived from the mother wavelet through its shifting and scaling. Recently, the wavelet analysis has been applied for structural health and fault monitoring. At the beginning of the century, Quek, Wang et.al applied continuous Gabor wavelet transform to the experimental data obtained by a piezoelectric sensor as a local non-destructive method for crack localization in beams with about two per cent error. However, the disadvantage of the approach is the dependence of the wavelet scale on sampling rate, filter frequency, length of the signal and edge effects [9]. Two years later, Gentile and Messina used continuous Gaussian wavelet transform for theoretical advantages to noisy and clean discrete vibrational data to detect open cracks in beams. The authors found out that certain boundary conditions can reduce effectiveness of two-dimensional maps in order to detect the damaged location. Moreover, they concluded that a fundamental mode shape is not more useful than higher modes, or vice versa, for damage detection. A comprehensive research required damages minor than 50 per cent thickness reduction [10]. Cao and Qiao studied cracks in null-thickness interface made of polymethyl methacrylate using a novel integrated biorthogonal spline wavelet transform that combines the advantages of the stationary and continuous wavelet transforms. The method showed robust results in identifying minor damage using a lower signal-to-noise ratio signal [11]. All the above cited papers are focused on a crack as damage detection.

The aim of the present paper is to develop a complex approach to delamination length or localization identification independent of boundary conditions. Haar wavelets have been chosen because of their ability to perform discrete wavelet transform and efficient preprocessing for deformation monitoring [8]. The technique has been supplied with machine learning methods for patterns classification and prediction.

For the last two decades, ANNs have frequently been used for finding a relationship between non-linearly dependable parameters or making predictions. Therefore, ANNs are considered a powerful tool for solving inverse problems [12]. However, ANNs require a large training data set, which is not always available or may contain coincidental values. In the present paper, it is suggested that the vibrating signal should first be filtered.

Recently, SVM has become one of the most intelligent classifiers with strong generalization ability [4]. The method is based on the statistical learning theory and is capable of processing a signal with a small number of samples. Due to the latter feature, SVMs have broadly been used in many practical applications: face recognition, time series forecasting, modeling of non-linear dynamic systems, etc. In the area of fault diagnosis, the application of SVM has not been extensively studied yet and requires future development [13]. According to P. Konar and P. Chattopadhyay, SVM along with advanced signal processing tools such as instantaneous power FFT, Park's transformation, bispectrum, wavelets will significantly improve the existing diagnostic systems [6].

In the present paper a new method for delamination identification in homogeneous and composite beams using vibration-based damage detection methods and real-time measured structural response signals i.e. mode shapes and modal frequencies is suggested. The limitations of the vibration analysis are solved by Haar wavelets and machine learning techniques such as SVMs and ANNs. Furthermore, the proposed compound approach is supposed to overcome the drawbacks of non-destructive testing systems, such as electrostatic field, X-ray, etc, and make trustworthy calculations. The novelty of the research consists in the utilization of SVMs for extraction of useful patterns from the signal for delamination detection. The patterns selected by SVMs are used for ANNs training. The paper is divided into six sections. Section two describes dynamic responses of vibrating beams. In Section three Haar wavelets are introduced. Section four provides an overview

of SVMs and selection of the most informative patterns from a data set. Section five describes the complex procedure for delamination identification. Various numerical examples can be found in section six.

2. DYNAMIC RESPONSE OF VIBRATING BEAMS WITH DELAMINATIONS

A vibrating system with n delaminations can be considered a combination of $3n + 1$ beam sections, connected at delamination boundaries (see Fig. 1).

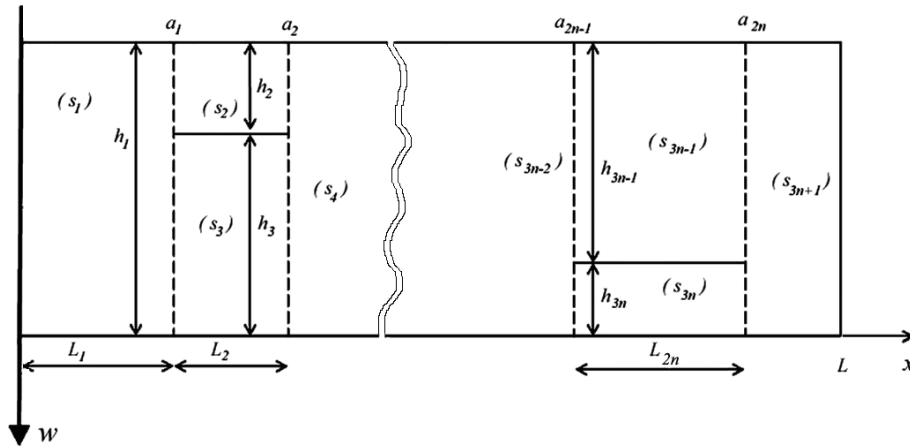


Fig. 1. A beam with n delaminations.

Each section is considered a classical Euler-Bernoulli beam with a constrained mode, rigid connector and bending-extension coupling [14]. The governing equation for the intact beam sections is

$$D_i \frac{\partial^4 w_i}{\partial x^4} + \rho_i A_i \frac{\partial^2 w_i}{\partial t^2} = 0, \quad (1)$$

where $i = 1, \dots, 3n + 1$; $w_i(x, t)$ is the vertical displacement of the i -th beam section; ρ_i is the density of material; A_i is the cross-sectional area; x is the axial coordinate, t is the time; D_i is the bending stiffness [14]. The formulas of D_i for composite beams can be found in [15]. The solution of (1) is sought in the form of:

$$w_i(x, t) = W_i(x) \sin(\omega t), \quad (2)$$

where ω is the natural frequency and $W_i(x)$ is the mode shape of the i -th beam section. Substituting (2) into (1), taking into account $x_i = x/L_i$ and eliminating a trivial solution of $\sin(\omega t) = 0$, the solution of Eq. (1) is as follows

$$W_i(x) = C_{i1} \sin(kx_i) + C_{i2} \cos(kx_i) + C_{i3} \sinh(kx_i) + C_{i4} \cosh(kx_i), \quad (3)$$

where

$$k_i^4 = \frac{\omega^2 \rho_i A_i L_i^4}{D_i} \quad (4)$$

and C_{i1}, \dots, C_{i4} are the arbitrary integrating constants. Hereof, the solution for the beam as a whole is a combination of the solutions of all the component beams enforced by the appropriate boundary and continuity conditions.

The boundary conditions at the supports $x = 0$ and $x = L$ are as follows. If the beam is clamped at $x = 0$, then $W_1 = 0$ and $W_1' = 0$; if simply supported, then $W_1 = 0$ and $W_1'' = 0$; if free, then

$W_1'' = 0$ and $W_1''' = 0$; if guided, then $W_1' = 0$ and $W_1'' = 0$. The analogous boundary conditions can be established at $x = L$.

The continuity conditions are applied at the boundaries of delaminations. In view of simplicity, consider the case $x = a_1$. The continuity conditions for deflection, slope and shear force at $x = a_1$ can be presented as:

$$\begin{aligned} W_1 &= W_2, \\ W_1' &= W_2', \\ D_1 W_1''' &= (D_2 + D_3) W_2'''. \end{aligned} \quad (5)$$

The continuity condition for the bending moments at the ends of delamination is presented as follows [14]

$$\begin{aligned} M_1 &= M_2 + M_3 - \frac{1}{2} P_3 (h_1 - h_3), \\ M_i &= -D_i W_i'', \end{aligned} \quad (6)$$

where $i = 1, 2, 3$. The axial forces P_2 and P_3 are established from the compatibility between stretching/shortening of the delaminated layers and axial equilibrium, which yield

$$\begin{aligned} \frac{P_3 L_2}{EA_1} - \frac{P_2 L_2}{EA_2} &= \left(W_1'(a_1) - W_4'(a_2) \right) \frac{h_1}{2}, \\ P_2 + P_3 &= 0, \end{aligned} \quad (7)$$

where a_1 denotes the coordinate of the cross-section between the section before delamination s_1 and the section with delamination s_2 , whereas a_2 is the coordinate between the beam section with delamination s_3 and the next intact section s_4 (Fig. 1).

3. HAAR WAVELETS

In recent years, the wavelet transform has occasionally been implemented in structural health monitoring. The advantage of the technique consists in the fact that the method does not require the analysis of the complete structure and has the ability to reveal some hidden parts of data that other signal analysis techniques fail to detect [17, 18]. In [19], it is demonstrated that the Haar wavelets can be applied for numerical solution of differential equations.

The Haar wavelet family is a group of square waves [19]:

$$h_i(x) = \begin{cases} 1 & \text{for } x \in \left[\frac{k}{m}, \frac{2k+1}{2m} \right], \\ -1 & \text{for } x \in \left[\frac{2k+1}{2m}, \frac{k+1}{m} \right], \\ 0 & \text{elsewhere.} \end{cases} \quad (8)$$

Integer m is the index of delay and it is equal to 2^j ; $j = 0, 1, \dots, J$ indicates the level of the wavelet; $k = 0, 1, \dots, m-1$ is the translation parameter. Integer J determines the maximal level of resolution. Index i is calculated according to formula $i = m + k + 1$. The minimal value for i is $i=2$; in this case $m = 1$, $k = 0$. The maximal value of i is $i = 2M = 2^{J+1}$. Value $i = 1$ corresponds to the scaling function for which $h_1(x) \equiv 1$.

Proceeding from the definition above, any function $y(x)$, which is square integrable in the interval $[0,1]$, can be expanded into a Haar series with an infinite number of terms:

$$y(x) = \sum_{i=0}^{\infty} c_i h_i(x), \quad (9)$$

where Haar coefficients are determined such that the integral square error ε is minimized

$$\varepsilon = \int_0^1 \left[y(x) - \sum_{i=1}^m c_i h_i(x) \right]^2 dx. \tag{10}$$

Any Haar function $h_i(x)$ can be calculated in collocation points: $x_l = (l - 0.5)/2M$, where $l = 1, 2, \dots, 2M$. Matrix $H(i, l) = h_i(x_l)$, which is associated with Haar wavelets, is obtained as follows:

$$H(i, l) = \begin{vmatrix} h_1(x_1) & \dots & h_1(x_{2M}) \\ \dots & \dots & \dots \\ h_{2M}(x_1) & \dots & h_{2M}(x_{2M}) \end{vmatrix} = H.$$

If function $y(x)$ is a piece-wise constant or it can be approximated as a piece-wise constant, the sum can be terminated as

$$y(x_l) = \sum_{i=1}^{2M} c_i h_i(x) = c_{2M}^t h_{2M}, \tag{11}$$

where the coefficient vector is

$$c_{2M}^t = y_{2M}^* H_{2M \times 2M}^{-1} \tag{12}$$

and

$$y_{2M}^* = [y(1/4M)y(3/4M)\dots y((4M - 1)/4M)]. \tag{13}$$

Both matrices H and H^{-1} are calculated once and contain zeros; therefore, the Haar transform works faster than Fourier transform.

The non-dimensional feature index vector of level l with $2M$ ($2M = 2^{l+1}$) components can be presented through the i th mode shape vectors $W_{i(2M)}^{*D}$ and $W_{i(2M)}^{*0}$ of the delaminated and the intact beam, respectively, as follows

$$P_i^l = (P_{i,1}^l, \dots, P_{i,2M}^l) = \frac{\left(W_{i(2M)}^{*D} - W_{i(2M)}^{*0} \right) H_{(2M \times 2M)}^{-1}}{\left\| \left(W_{i(2M)}^{*D} - W_{i(2M)}^{*0} \right) H_{(2M \times 2M)}^{-1} \right\|}, \tag{14}$$

where $\| \cdot \|$ is the Euclidean norm.

In the present study, the Haar wavelet transform is applied to the first mode shape of the intact and delaminated beam. The choice of the mode shape was based on the results of Cao et al. [20]. The sensitivity analysis of the present Haar wavelet approach was carried out in [16].

4. INTEGRATION OF SUPPORT VECTOR MACHINES

If a system is linear, it is relatively easy to find the relationship between characteristic parameters. Conversely, if a system is non-linear, the mapping task requires optimization. For that reason, SVMs are used in the present research paper on vibrating beams with delaminations in order to ease the task of ANNs on learning from the observed data.

SVM is a supervised learning algorithm for pattern classification and regression based on the statistical learning theory [4]. In the cases where a small number of samples are available, the method is capable of mapping non-linear functions quite efficiently. The main advantages of the technique are the following: SVM seeks for the global optimized solution and avoids over-fitting.

Such a powerful classification tool was developed by Vapnik in the mid 1990s; in recent years, it has widely been used in real-world applications such as face recognition, time series forecasting, biosequence analysis, text categorization, and fault detection because of their high accuracy. In the field of damage diagnostics, the tool is still pioneering yet [6].

The main idea of SVMs is to classify data into two classes in the following way. First, SVM puts a separating hyperplane between the data points in the feature space; then it orientates itself in such a way that the margin is maximized; most of the data points of the same class are allocated on the same side. As a result, generalization is performed with the least error, and the data is divided into two classes (the latter concept can be extended to multi-class problems) [21]. The points that form the margin are called support vectors; they define the classifier. The main concepts of SVMs are presented graphically in Fig. 2.

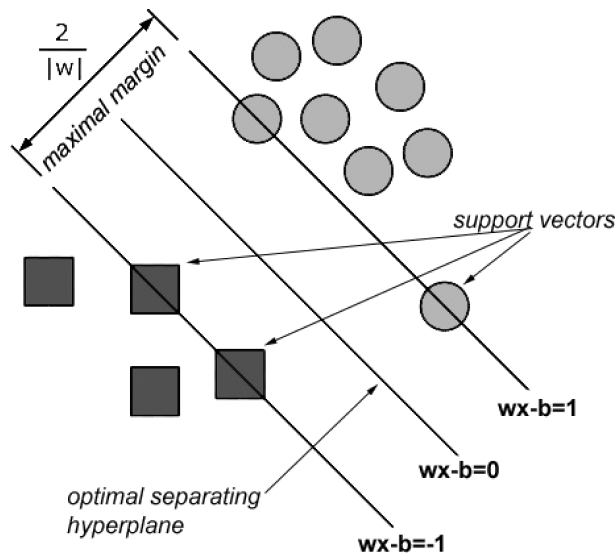


Fig. 2. An optimal hyperplane.

Consider a sample training set (x_i, y_i) , where $x_i \in \mathbb{R}^n$ is the training data, $y_i \in \{-1, 1\}$ is the class of labels for x_i, \dots, x_N (N is the total number of samples). The hyperplane $f(x) = 0$ that separates the data into two classes is a solution to the convex quadratic optimization problem:

$$\begin{aligned} & \text{minimize } \frac{1}{2} \|w\|^2, \\ & \text{subject to } y_i(w^T x_i + b) \geq 1, \quad i = 1, \dots, N, \end{aligned} \quad (15)$$

where w is the orientation vector and b is the location parameter, respectively. If data to be classified is non-linearly separable, it is mapped using a non-linear transfer function onto a high-dimensional feature space, where the linear classification is possible.

Once the algorithm is trained, it can be tested with new data patterns. For any new set of data, SVM uses w and b to predict the class to which the set should belong [22]. A more detailed description of SVMs can be found in [23].

5. DELAMINATION IDENTIFICATION IN BEAMS USING HAAR WAVELETS, SVM AND ANN

In the present research paper on delamination detection in vibrating systems, a novel complex approach has been developed. SVM along with advanced signal processing tools such as NNs and Haar wavelets have been applied. The whole process is shown in Fig. 3. Initially, the first mode shape

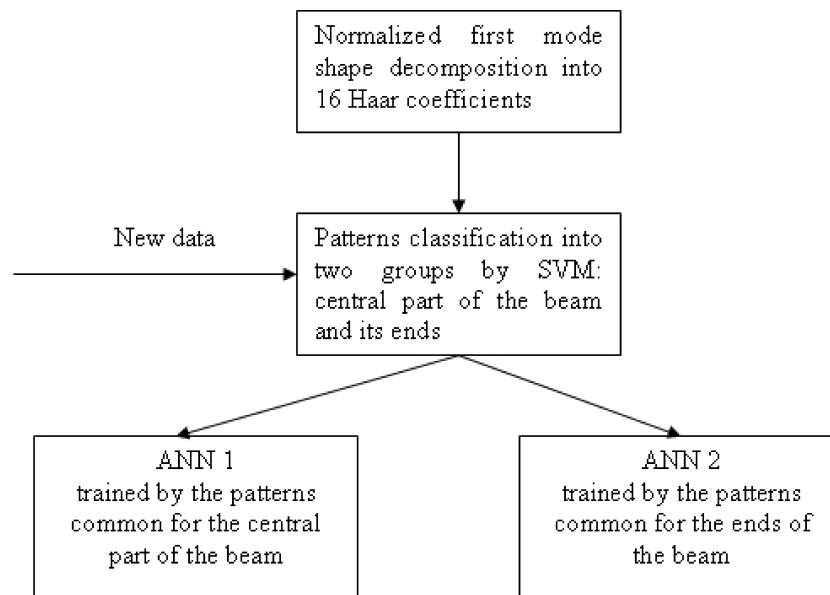


Fig. 3. The delamination detection system.

is normalized and converted into sixteen Haar coefficients (resolution J is equal to three) [16]. Then the data is classified into two classes by SVM. The patterns that characterize small delaminations or small distances are allocated into the first class; the other patterns are placed into the second class. SVM is trained by the quadratic transfer function. Once the data is classified, it is used for training two ANNs with different architecture. Generally, the number of hidden layers depends on the number of parameters to be predicted; the number of neurons on each layer has been dictated by the number of training patterns. The learning algorithm is Bayesian since it has come up with precise results in the previous research [16]. Once the system is trained, it is ready for testing. When a new mode shape is extracted, it is transformed into Haar coefficients, then processed by SVM and fed into the appropriate ANN in order to calculate the location and/or size of delamination. All the numerical calculations have been carried out in the Matlab environment.

6. NUMERICAL EXAMPLES

First, the suggested approach for delamination detection was applied to a homogeneous beam with clamped ends. The system predicted the length of delamination which occurred in the midplane of the beam. SVM divided 190 training patterns into two groups: large delamination and a small one (less than ten percent). After the SVM classification, there were 154 patterns in the first class and 36 patterns in the other one. Each training pattern contained six frequencies or 16 Haar coefficients. Table 1 shows the actual length of delamination, the lengths calculated by the systems with or without SVM or Haar coefficients. Coefficient of multiple determination $R^2 = 1 - \frac{\sum(n_t - n_p)^2}{\sum(n_t - n_m)^2}$ presents the closeness of fit. In the formula n_t and n_p denote the target and computed value, respectively; n_m is the mean of the target values n_t . Ideally, R^2 is equal to 1. In Table 1, it is seen that the methods based on frequencies are more accurate than the ones based on Haar wavelets. SVMs have not influenced the accuracy of the calculations.

Second, the proposed method was examined on a homogenous cantilever with two delaminations in the midplane each ten percent large. The system predicted the distance from the left end of the beam to the first delamination (D_1) and the distance between two delaminations (D_2). SVM divided 177 training patterns into two groups: 89 patterns were set into the first class in which at least one of the distances was smaller than 12 percent; the remaining patterns were allocated into the other class. The results of the predictions are provided in Table 2.

Table 1. Delamination length prediction in a homogeneous beam with clamped ends.

| Actual length | Using 6 frequencies | Using frequencies and SVM | Using 16 Haar coefficients | Using SVM and Haar coefficients |
|---------------|---------------------|---------------------------|----------------------------|---------------------------------|
| 0.0110 | 0.0094 | 0.0105 | 0.0188 | 0.0207 |
| 0.0380 | 0.0377 | 0.0379 | 0.0379 | 0.0383 |
| 0.0510 | 0.0506 | 0.0505 | 0.0510 | 0.0514 |
| 0.0860 | 0.0856 | 0.0855 | 0.0858 | 0.0869 |
| 0.1510 | 0.1507 | 0.1507 | 0.1568 | 0.1510 |
| 0.2030 | 0.2032 | 0.2033 | 0.2030 | 0.2027 |
| 0.2610 | 0.2609 | 0.2607 | 0.2611 | 0.2610 |
| 0.3260 | 0.3257 | 0.3257 | 0.3260 | 0.3260 |
| 0.3960 | 0.3957 | 0.3957 | 0.3959 | 0.3960 |
| 0.4830 | 0.4835 | 0.4833 | 0.4831 | 0.4830 |
| R^2 | 1.0000 | 1.0000 | 0.9996 | 0.9996 |

Table 2. Distance to the first delamination and between two delaminations in a homogenous cantilever.

| Actual length | | Using 6 frequencies | | Using frequencies and SVM | | Using 16 Haar coefficients | | Using SVM and Haar coefficients | |
|---------------------|--------|---------------------|--------|---------------------------|--------|----------------------------|--------|---------------------------------|--------|
| D_1 | D_2 | D_1 | D_2 | D_1 | D_2 | D_1 | D_2 | D_1 | D_2 |
| 0.0300 | 0.1100 | 0.0154 | 0.1984 | 0.0860 | 0.1057 | 0.0224 | 0.1731 | 0.0306 | 0.1739 |
| 0.0300 | 0.6700 | 0.1630 | 0.3774 | 0.1760 | 0.4849 | 0.0320 | 0.6823 | 0.0334 | 0.6475 |
| 0.1100 | 0.5900 | 0.0005 | 0.5028 | 0.2235 | 0.2914 | 0.1142 | 0.5555 | 0.1062 | 0.5298 |
| 0.1900 | 0.0700 | 0.1537 | 0.3944 | 0.3096 | 0.3075 | 0.1665 | 0.0717 | 0.1888 | 0.0541 |
| 0.1900 | 0.5100 | 0.1100 | 0.6463 | 0.1688 | 0.4414 | 0.1942 | 0.4949 | 0.1948 | 0.4976 |
| 0.2700 | 0.1100 | 0.2857 | 0.0708 | 0.2235 | 0.2914 | 0.2436 | 0.0778 | 0.2520 | 0.1017 |
| 0.3400 | 0.4300 | 0.4876 | 0.1915 | 0.2235 | 0.2914 | 0.3274 | 0.4394 | 0.3356 | 0.4415 |
| 0.4200 | 0.3100 | 0.4067 | 0.3350 | 0.3096 | 0.3075 | 0.4168 | 0.3134 | 0.4202 | 0.3109 |
| 0.4600 | 0.1500 | 0.3611 | 0.4194 | 0.3096 | 0.1572 | 0.5068 | 0.1279 | 0.4420 | 0.1505 |
| R^2 | | 0.7042 | 0.1503 | 0.4874 | 0.4400 | 0.9815 | 0.9830 | 0.9916 | 0.9791 |
| R^2_{mean} | | 0.4273 | | 0.4637 | | 0.9823 | | 0.9854 | |

Third, the proposed method was examined on a composite beam: T300/934 graphite/epoxy beam with a $[0^0/90^0]_{2s}$ stacking sequence. The dimensions of an 8-ply beam are $127 \times 12.7 \times 1.016 \text{ mm}^3$. The material properties for the lamina are $E_{11} = 134 \text{ GPa}$; $E_{22} = 10.3 \text{ GPa}$; $G_{12} = 5 \text{ GPa}$; $\nu_{12} = 0.33$ and $\rho = 1.48 \times 10^3 \text{ kg/m}^3$ [24, 25]. The system computed the length of delamination located between the first and the second plies of the cantilever. Table 3 shows the results of the predictions. They are quite similar to the first example. The simpler methods, without using Haar wavelets, produced the most precise results.

Finally, a composite beam with simply supported ends and a growing delamination between the first and the second plies was investigated. The system predicted the location of delamination from the left end of the beam (L_1) and the length of delamination (L_2). The results are presented in Table 4.

Negative R^2 stands for the fact that no firm relationship between input and output data was found, and the ANNs made irrelevant predictions. Comparing the coefficients, it is seen that the aggregated approach of Haar wavelets and SVMs made the most accurate predictions.

Table 3. Delamination length prediction in a composite cantilever.

| Actual length | Using 6 frequencies | Using frequencies and SVM | Using 16 Haar coefficients | Using SVM and Haar coefficients |
|---------------|---------------------|---------------------------|----------------------------|---------------------------------|
| 0.0046 | 0.0046 | 0.0046 | 0.0045 | 0.0046 |
| 0.0094 | 0.0094 | 0.0094 | 0.0092 | 0.0094 |
| 0.0124 | 0.0124 | 0.0124 | 0.0126 | 0.0123 |
| 0.0184 | 0.0184 | 0.0184 | 0.0181 | 0.0183 |
| 0.0232 | 0.0232 | 0.0232 | 0.0233 | 0.0235 |
| 0.0274 | 0.0274 | 0.0274 | 0.0268 | 0.0267 |
| 0.0394 | 0.0394 | 0.0394 | 0.0394 | 0.0393 |
| 0.0556 | 0.0556 | 0.0556 | 0.0555 | 0.0557 |
| 0.0796 | 0.0796 | 0.0796 | 0.0797 | 0.0797 |
| 0.1129 | 0.1120 | 0.1120 | 0.1119 | 0.1114 |
| R^2 | 1.0000 | 1.0000 | 0.9999 | 0.9999 |

Table 4. Distance to the first delamination and length of the first delamination in a beam with simply supported ends.

| Actual length | | Using 6 frequencies | | Using frequencies and SVM | | Using 16 Haar coefficients | | Using SVM and Haar coefficients | |
|---------------------|--------|---------------------|--------|---------------------------|--------|----------------------------|--------|---------------------------------|--------|
| L_1 | L_2 | L_1 | L_2 | L_1 | L_2 | L_1 | L_2 | L_1 | L_2 |
| 0.0010 | 0.0460 | 0.0348 | 0.0438 | 0.0411 | 0.0439 | 0.0439 | 0.0516 | 0.0041 | 0.0408 |
| 0.0080 | 0.0160 | 0.0393 | 0.0151 | 0.1625 | 0.0146 | 0.0493 | 0.0095 | 0.0070 | 0.0141 |
| 0.0150 | 0.0040 | 0.0455 | 0.0058 | 0.0473 | 0.0060 | 0.0128 | 0.0041 | 0.0140 | 0.0039 |
| 0.0150 | 0.0460 | 0.0592 | 0.0458 | 0.0402 | 0.0459 | 0.0054 | 0.0386 | 0.0142 | 0.0410 |
| 0.0290 | 0.0100 | 0.0731 | 0.0085 | 0.0570 | 0.0095 | 0.0428 | 0.0094 | 0.0340 | 0.0105 |
| 0.0290 | 0.0220 | 0.1450 | 0.0198 | 0.0517 | 0.0211 | 0.0210 | 0.0236 | 0.0287 | 0.0224 |
| 0.0360 | 0.0160 | 0.0730 | 0.0167 | 0.0543 | 0.0154 | 0.0421 | 0.0163 | 0.0343 | 0.0166 |
| 0.0360 | 0.0520 | 0.0381 | 0.0519 | 0.0365 | 0.0538 | 0.0336 | 0.0511 | 0.0348 | 0.0519 |
| 0.0710 | 0.0040 | 0.0599 | 0.0057 | 0.0580 | 0.0075 | 0.0732 | 0.0045 | 0.0709 | 0.0049 |
| 0.0780 | 0.0460 | 0.0326 | 0.0448 | 0.0405 | 0.0452 | 0.1650 | 0.0166 | 0.0759 | 0.0440 |
| R^2 | | -3.1307 | 0.9937 | -4.2341 | 0.9916 | -0.9847 | 0.6994 | 0.9921 | 0.9815 |
| R^2_{mean} | | -1.0685 | | -1.6213 | | -0.1427 | | 0.9868 | |

7. CONCLUDING REMARKS

The main objective of the present research paper was to develop a novel method for delamination detection in homogeneous and composite beams. Since delamination influences significantly the frequency domain of vibrating systems, the new approach was based on mode shapes. To make the data more sensitive and qualitative, the first mode shape was normalized and converted into 16 Haar coefficients. The feature parameters were predicted by contemporary computational methods: SVM, a tool for pattern recognition and classification, and ANN, a tool for establishing relationship between the input and output data. SVMs were expected to select the most informative data from the data set. The latter method divided the training patterns into two classes: patterns that characterize small distances or delaminations, and the remaining patterns. According to the classes, two ANNs of different architecture were created and trained by the corresponding class of patterns. The proposed aggregated method was examined on four different physical models. The results showed that if only one parameter is to be calculated, the computational method can be simple:

frequency-based patterns and ANNs. In such cases, the use of SVMs do not influence the accuracy of the predictions while the Haar wavelets reduce it. If two parameters are to be predicted, the composite approach of Haar wavelets, SVMs and ANNs provide the most accurate values.

ACKNOWLEDGEMENTS

Financial support from the Estonian Science Foundation under Grant ETF 8830 and the project SF0180008s12 are gratefully acknowledged.

REFERENCES

- [1] I. Payo, J.M. Hale. Sensitivity analysis of piezoelectric paint sensors made up of PZT ceramic powder and water-based acrylic polymer. *Sensors and Actuators A, Physical*, **168**: 77–89, 2011.
- [2] R. Ly, M. Rguiti, S. D’Astorg, A. Hajjaji, C. Courtois, A. Leriche. Modeling and characterization of piezoelectric cantilever bending sensor for energy harvesting. *Sensors and Actuators A, Physical*, **168**: 95–100, 2011.
- [3] R. Teti, K. Jemielniak, G. O’Donnell, D. Dornfeld. Advanced monitoring of machining operations. *CIRP Annals – Manufacturing Technology*, **59**: 717–739, 2010.
- [4] L.M.R. Baccarini, V.V.R. e Silva, B.R. de Menezes, W.M. Caminhas. SVM practical industrial application for mechanical faults diagnostic. *Expert Systems with Applications*, **38**: 6980–6984, 2011.
- [5] N.R. Fisco, H. Adeli. Smart structures: Part II – Hybrid control systems and control strategies. *Scientia Iranica*, **18**(3): 285–295, 2011.
- [6] P. Konar, P. Chattopadhyay. Bearing fault detection of induction motor using wavelet and Support Vector Machines (SVMs). *Applied Soft Computing*, **11**: 4203–4211, 2011.
- [7] A.N. Robertson, B. Basu. Wavelet Analysis. *Encyclopedia of Structural Health Monitoring*. John Wiley & Sons, Ltd., 2009.
- [8] M.M.R. Taha, A. Noureldin, J.L. Lucero, T.J. Baca. Wavelet Transform for Structural Health Monitoring: A Compendium of Uses and Features. *Structural Health Monitoring*, **5**: 267–295, 2006.
- [9] S.T. Quek, Q. Wnag, L. Zhang, K.H. Ong. Practical issues in the detection of damage in beams using wavelets. *Smart Materials and Structures*, **10**: 1009–1017, 2001.
- [10] A. Gentile, A. Messina. On the continuous wavelet transforms applied to discrete vibrational data for detecting open cracks in damaged beams. *International Journal of Solids and Structures*, **40**: 295–315, 2003.
- [11] M. Cao, P. Qiao. Integrated wavelet transform and its application to vibration mode shapes for the damage detection of beam-type structures. *Smart Materials and Structures*, **17**: 1–17, 2008.
- [12] Z. Waszczyszyn, L. Ziemianski. Neurocomputing in the analysis of selected inverse problems of mechanics of structures and materials. *Computer Assisted Mechanics and Engineering Sciences*, **13**: 125–159, 2006.
- [13] A. Widodo, B.S. Yang. Support vector machine in machine condition monitoring and fault diagnosis. *Mechanical Systems and Signal Processing*, **21**: 2560–2574, 2007.
- [14] P.M. Mujumdar, S. Suryanarayan. Flexural vibrations of beams with delaminations. *Journal of Sound and Vibration*, **125**: 441–461, 1988.
- [15] J.N. Reddy. *Mechanics of laminated composite plates*. CRC Press, 1997.
- [16] H. Hein, L. Feklistova. Computationally efficient delamination detection in composite beams using Haar wavelets. *Mechanical Systems and Signal Processing*, **25**: 2257–2270, 2011.
- [17] S.T. Quek, Q. Wang, L. Zhang, K.K. Ang. Sensitivity analysis of crack detection in beams by wavelet technique. *International Journal of Mechanical Sciences*, **43**: 2899–2910, 2001.
- [18] Y.J. Yan, L. Cheng, Z.Y. Wu, L.H. Yam. Development in vibration-based structural damage detection technique. *Mechanical Systems and Signal Processing*, **21**: 2198–2211, 2007.
- [19] Ü. Lepik. Numerical solution of differential equations using Haar wavelets. *Mathematics and Computers in Simulation*, **68**: 127–143, 2005.
- [20] M. Cao, L. Ye, L. Zhou, Z. Su, R. Bai. Sensitivity of fundamental mode shape and static deflection for damage identification in cantilever beams. *Mechanical Systems and Signal Processing*, **25**: 630–643, 2010.
- [21] K. Salahshoor, M. Kordestani, M. Khoshro. Fault detection and diagnosis of an industrial steam turbine using fusion of SVM (support vector machine) and ANFIS (adaptive neuro-fuzzy inference system) classifiers. *Energy*, **35**: 5472–5482, 2010.
- [22] V. Sugumaran, K. Ramachandran. Effect of number of features on classification of roller bearing faults using SVM and PSVM. *Expert Systems with Applications*, **38**: 4088–4096, 2011.
- [23] V.N. Vapnik. *The nature of statistical learning theory*. Springer, Berlin, 1995.
- [24] M.H.H. Shen, J.E. Grady. Free vibrations of delamination beams. *AIAA Journal*, **30**: 1361–1370, 1992.
- [25] D. Shu, C.N. Della. Free vibration analysis of composite beams with two non-overlapping delaminations. *International Journal of Mechanical Sciences*, **46**: 509–526, 2004.